

Gold particles supported on self-organized nanotubular TiO₂ matrix as highly active catalysts for electrochemical oxidation of glucose

Mirghasem Hosseini · Mohamad Mohsen Momeni

Received: 4 May 2009 / Revised: 2 August 2009 / Accepted: 10 August 2009 / Published online: 29 August 2009
© Springer-Verlag 2009

Abstract Au/TiO₂/Ti electrode was prepared by a two-step process of anodic oxidation of titanium followed by cathodic electrodeposition of gold on resulted TiO₂. The morphology and surface analysis of Au/TiO₂/Ti electrodes was investigated using scanning electron microscopy and EDAX, respectively. The results indicated that gold particles were homogeneously deposited on the surface of TiO₂ nanotubes. The nanotubular TiO₂ layers consist of individual tubes of about 60–90 nm in diameter, and the electrode surface was covered by gold particles with a diameter of about 100–200 nm which are distributed evenly on the titanium dioxide nanotubes. This nanotubular TiO₂ support provides a high surface area and therefore enhances the electrocatalytic activity of Au/TiO₂/Ti electrode. The electrocatalytic behavior of Au/TiO₂/Ti electrodes in the glucose electro-oxidation was studied by cyclic voltammetry. The results showed that Au/TiO₂/Ti electrodes exhibit a considerably higher electrocatalytic activity toward the glucose oxidation than that of gold electrode.

Keywords Au/TiO₂/Ti electrode · Titanium dioxide · Nanotube · Electrocatalysis · Glucose oxidation

Introduction

Determination of glucose has been investigated most extensively as the target analyte in diagnosis of diabetes. Most previous studies on this subject involved the use of

the enzyme “glucose oxidase” (GODx) [1–4], which catalyzes the oxidation of glucose to gluconolactone. However, due to the intrinsic nature of enzymes, such enzyme-based sensors have some stability problems. For example, the activity of GODx can be easily affected by temperature, pH, humidity, and toxic chemicals [5]. To overcome this obstacle, attempts have been made to develop other suitable sensory systems [6–10]. The direct electrochemical oxidation of glucose on different substrates such as platinum [6–8] and alloys (containing Pt, Pb, Au, Pd, and Rh) [11] has been explored in the hope of developing effective enzyme-free sensors. However, these conventional electrodes have some disadvantages, such as low sensitivity and poor selectivity, caused by surface poisoning due to adsorbed intermediates and chloride ions [12]. Gold has long been known as being catalytically far less active than other transition metals [13]. As a consequence, gold is not expected to be a good candidate for catalytic oxidation or hydrogenation processes. However, this lack of reactivity seems to be a characteristic of pure gold since some catalyst preparations, where the metallic particles are supported on oxides, have been reported to be highly active especially at room temperature. Immobilization of the noble metal particles in an active matrix may enhance the overall reactivity of the catalytic metal centers [14–23]. For example, our previous studies on the electrocatalytic oxidation of glycerol and evolution of chlorine on Pt/TiO₂ electrode has shown that the modification of electrode surface by anodization of titanium improves the electrocatalytic activity toward glycerol oxidation, as well as chloride oxidation to chlorine gas to a great extent [24,25]. Study of electrochemical glucose on gold nanoparticle has been reported by some authors [26–28]; glucose oxidation is a self-poisoning reaction which blocks the active electrocatalyst surface by strongly adsorbed

M. Hosseini (✉) · M. M. Momeni
Electrochemistry Research Laboratory, Department of Physical
Chemistry, Chemistry Faculty, University of Tabriz,
Tabriz, Iran
e-mail: mg-hosseini@tabrizu.ac.ir

reaction intermediates such as CO, the efficiency of the electrodes reduces due to poisoning of the catalyst, and relatively poor mass-specific power densities are obtained. Therefore, it is necessary to place more emphasis on electrocatalyst research and to attain a significantly higher power density. To improve the oxidation rate and electrode stability, considerable efforts have been applied to the study of electrode materials. In these studies, some economical materials, including graphite, glass carbon, and novel materials such as carbon nanotubes were used as substrate for dispersing catalytic metal particles. In the present work, in order to obtain a high surface area support, the Au particles were brought onto a nanotubular TiO₂ matrix. In this research, Au/TiO₂/Ti electrode was fabricated by anodization of the titanium substrate to produce TiO₂ nanotubes with subsequent filling of the nanotubular TiO₂ by cathodic deposition of gold. Self-organized TiO₂ films were formed in 1 M Na₂SO₄+0.5 wt.% NaF. Then, deposition of gold took place under galvanostatic conditions from a cyanide bath containing KAu(CN)₂ in the presence of a citrate buffer. The electrochemical catalytic activities of the Au and Au/TiO₂/Ti electrodes in electro-oxidation of glucose in basic aqueous solutions were investigated. The morphology of the titanium oxide films and gold coating on titanium oxide films were studied with a scanning electron microscope (Philips Model XL30) and energy-dispersive X-ray spectroscopy (EDAX).

Experimental

Reagents

All chemicals were of analytic purity grade and used without further purification. All aqueous solutions were prepared with distilled water.

Preparation of Au/TiO₂/Ti electrodes

Au/TiO₂/Ti electrode was prepared by a two-step process through anodic oxidation followed by cathodic gold electrodeposition. Titanium plates were cut from a titanium sheet (99.99% purity, 1-mm thick) and mounted using epoxy resin. Prior to anodization, the titanium electrodes were first mechanically polished with different emery type abrasive papers, rinsed in a bath of distilled water, and then chemically etched by immersing in a mixture of HF and HNO₃ acids for 1 min. The ratio of components HF/HNO₃/H₂O in the mixture was 1:4:5 in volume. The last step of pretreatment was rinsing with acetone and deionized water. After the pretreatment, the nanotubular TiO₂ were prepared by anodizing. Anodizing of titanium carried out in 1 M Na₂SO₄+0.5 wt.% NaF mixture solution at a constant

voltage of 20 V for 120 min at room temperature. After rinsing with water, the plates with nanotubular TiO₂ (TiO₂/Ti electrodes) were immersed into the gold electrodeposition bath. Deposition of gold within nanotubular TiO₂, took place under galvanostatic conditions. For gold deposition, the conditions were a current density of 10 mA cm⁻² for 10 min, in a cyanide bath containing KAu(CN)₂ in the presence of a citrate buffered with pH4. The temperature of bath is maintained at 45°C.

Physical characterization

Morphology, alignment, and composition of the TiO₂ nanotube array and gold coating on nanotubular TiO₂ films were characterized with a Philips scanning electron microscope (SEM) and EDAX.

Electrochemical experiments

All electrochemical experiments were carried out in a conventional three-electrode cell. The measuring equipment was a Princeton Applied Research, EG&G PARSTAT 2263 advanced potentiostat run by PowerSuite software. The reference electrode was a saturated calomel electrode (SCE). A platinum sheet with about 20 cm² geometric area was used as counter electrode. All potentials were measured with respect to SCE.

Results and discussion

Characterization of the electrodes morphology

The SEM images of the titanium dioxide nanotubes and the Au/TiO₂/Ti electrode is showed in Fig. 1. Figure 1a shows the SEM image of the titanium dioxide nanotubes prepared by anodic oxidation and the average tube diameter was about 60–90 nm, which can be used as good carrier of particle catalyst. It can be observed from Fig. 1b that the electrode surface was covered by gold particles with a diameter of about 100–200 nm which are distributed evenly on the titanium dioxide nanotubes. Figure 2 shows the energy dispersive X-ray spectrum of Au/TiO₂/Ti after a 10-min electroplating of gold on anodized titanium. Energy dispersive spectroscopy (EDS) results confirm the presence of gold on TiO₂ nanotubes.

Determination of electrode surface area

In order to compare prepared electrodes with pure gold electrode and to electrochemically characterize the real surface of the Au/TiO₂/Ti electrode, the area of the electrode was determined using 1 mM K₄Fe(CN)₆ in

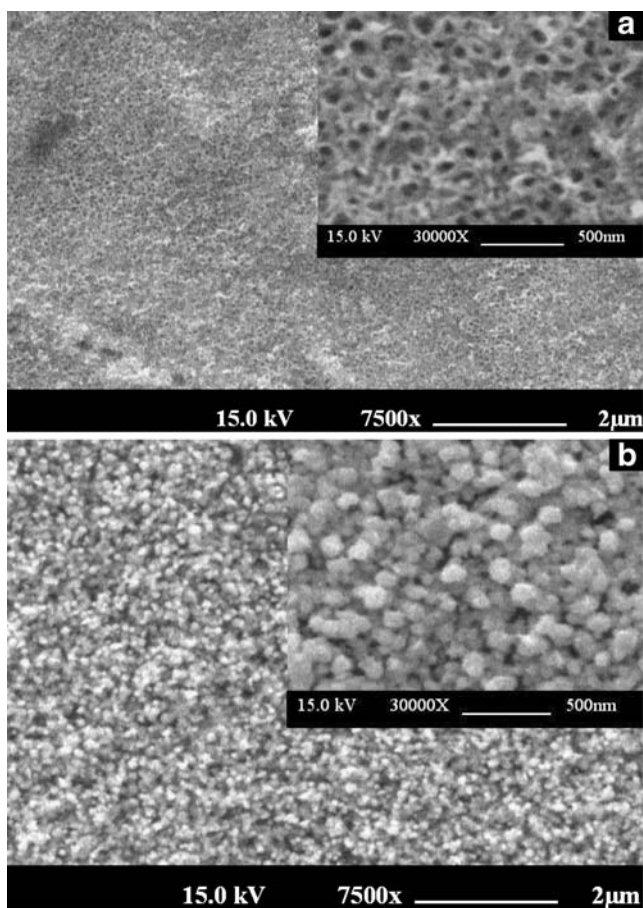
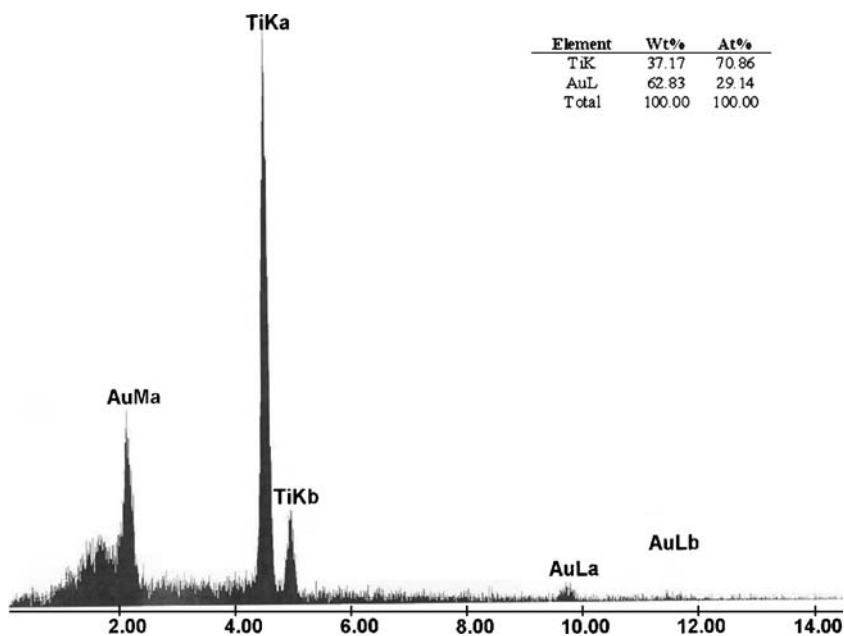


Fig. 1 **a** The surface morphology of the titanium dioxide nanotubes prepared by anodic oxidation, and **b** the surface morphology of gold coating on the Au/TiO₂/Ti electrode

Fig. 2 EDX of Au/TiO₂/Ti electrode (after 10-min electroplating of gold on anodized titanium)



0.1 M KNO₃ by recording the cyclic voltammograms. From the cyclic voltammetric peak current and the diffusion coefficient of hexacyanoferrate, the area of the electrode was calculated by using the Eq. (1) [29,30]:

$$i_{pa} = (2.69 \times 10^5) n^{3/2} A D_o^{1/2} \nu^{1/2} C_o^* \quad (1)$$

Where; *n* is the number of electrons transferred, i.e., 1, *A* is the surface area of the electrode, *D_o* is the diffusion coefficient (9.382 × 10⁻⁶ cm² s⁻¹), *ν* is the scan rate (0.1 V s⁻¹), *C_o*^{*} is the concentration of electro-active species (1 mM). The surface area of Au/TiO₂/Ti electrode was estimated to be about 40 times as that of Au electrode. Figure 3 shows the cyclic voltammograms obtained for Au/TiO₂/Ti and gold electrodes. The voltammograms for Au/TiO₂/Ti electrodes are not quantitatively similar to those for smooth polycrystalline gold; this indicates that the activity of Au/TiO₂/Ti electrodes is much more than of gold electrode.

Electro-oxidation of glucose

Cyclic voltammetric study of glucose electro-oxidation on the electrodes

In order to compare Au/TiO₂/Ti electrode with flat gold electrode, the method of cyclic voltammetry was used to estimate the electrocatalytic behavior of the electrodes in alkaline medium. Figure 4 presents cyclic voltammograms of gold and Au/TiO₂/Ti electrodes in 1 M NaOH solution recorded at a scan rate of 100 mV s⁻¹. It is evident from Fig. 4 that both the hydroxide ion adsorption and oxygen evolution peak current densities on Au/TiO₂/Ti electrode

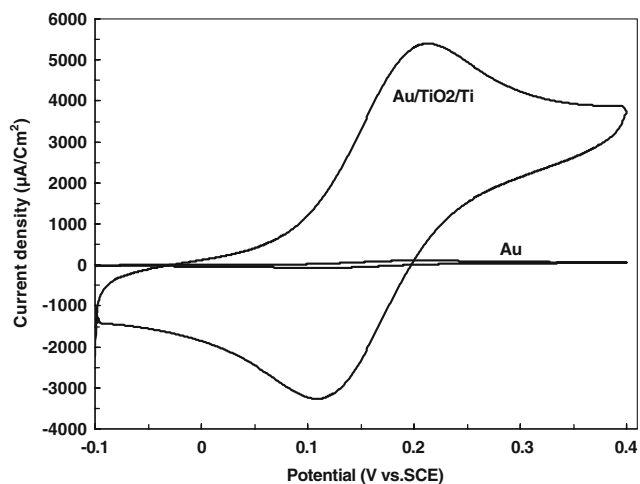


Fig. 3 Cyclic voltammograms for a Au/TiO₂/Ti and gold electrodes recorded at 100 mV s⁻¹ in a solution containing 1 mM K₄[Fe(CN)₆] in 0.1 M KNO₃ at 25°C

are higher than that of the flat gold electrode. Figure 5a, b show cyclic voltammograms of Au/TiO₂/Ti and gold electrodes in 1 M NaOH+0.01 M glucose aqueous solution, at a scan rate of 100 mV s⁻¹, respectively. The current density for glucose oxidation on Au/TiO₂/Ti electrode is greater than that observed for gold electrode. This result may also be attributed to the larger specific surface area of the Au/TiO₂/Ti electrodes. In addition, to clarify if the increase of the specific area is the only factor to explain the increase of the oxidation current or the modification of the electrode provides new reaction pathways, decreasing the activation energy barrier of the reaction; the temperature dependency of glucose oxidation on Au/TiO₂/Ti and Au electrodes were investigated in the temperature range of 20–80°C by the method of cyclic voltammetry and it was

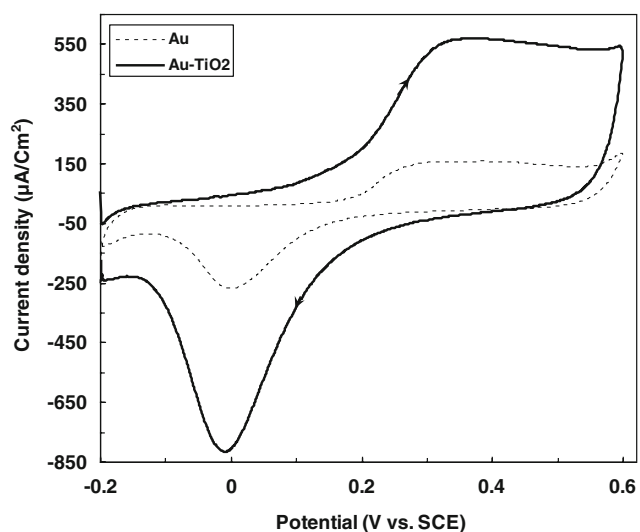


Fig. 4 Cyclic voltammograms for Au/TiO₂/Ti and gold electrodes in a 1 M NaOH solution at 25°C with a scan rate of 100 mV s⁻¹

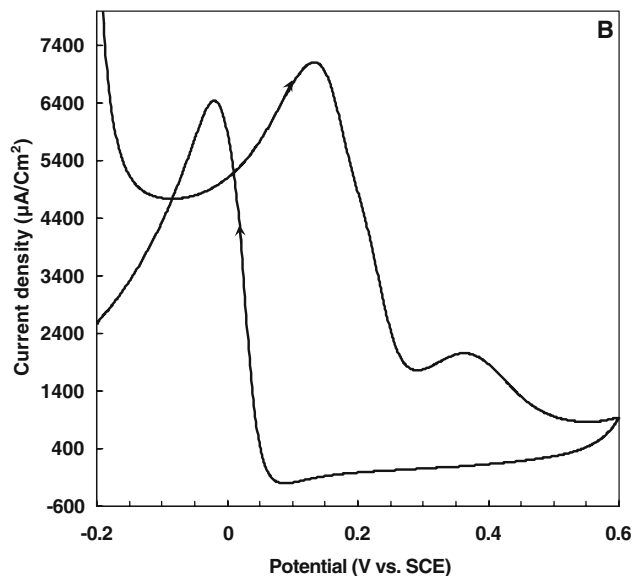
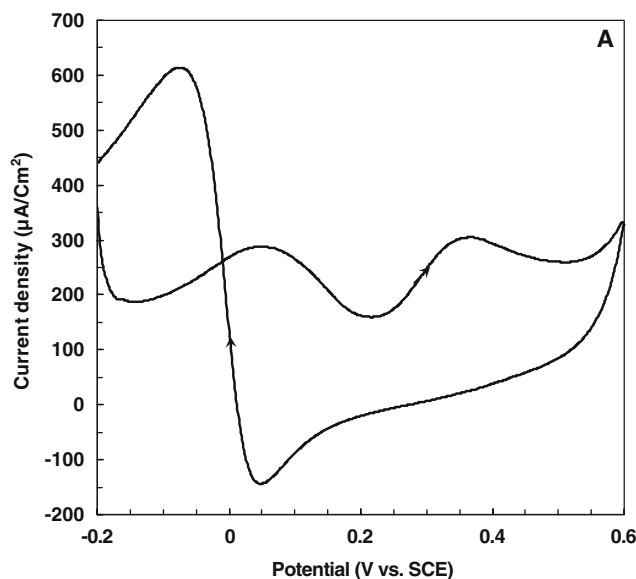


Fig. 5 Cyclic voltammograms for gold electrode (a) and Au/TiO₂/Ti electrode (b) in a 1 M NaOH–0.01 M glucose aqueous solution at 25°C with a scan rate of 100 mV s⁻¹

seen that anodic current increased with temperature increase. Arrhenius plots for the anodic current of glucose oxidation on Au/TiO₂/Ti and Au electrodes showed a linear correlation is obtained between $\ln i$ and $1/T$, the apparent activation energy for Au/TiO₂/Ti electrode was found to be lower than Au electrode. Thus increasing of the specific area and decreasing of activation energy for are two parameters that increased the oxidation current.

Continuous Cyclic voltammetric properties of glucose on Au/TiO₂/Ti and gold electrodes

Figures 6 and 7 show the continuous cyclic voltammetric curves of glucose at pure gold and Au/TiO₂/Ti electrodes,

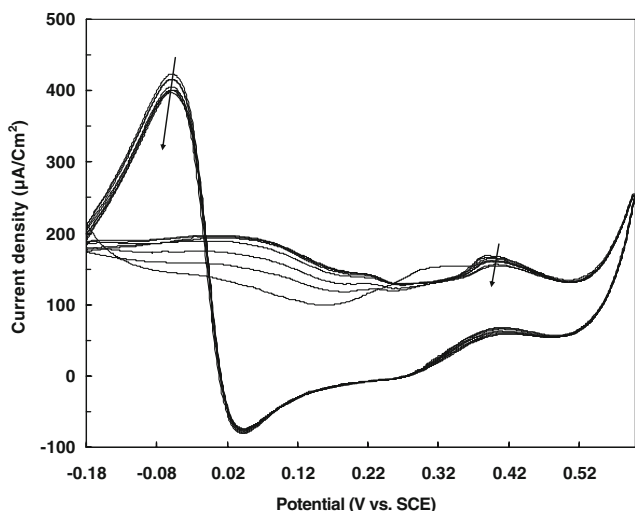


Fig. 6 The continuous cyclic voltammograms of glucose on gold electrode in a 1 M NaOH–0.01 M glucose aqueous solution at 25°C with a scan rate of 50 mV s⁻¹

respectively. It is seen from Fig. 6 that the oxidation peak current density of glucose on pure gold electrode is decreasing in subsequent scan cycles. It can probably be due to the formation intermediates such as carbon monoxide adsorbed on the electrode in the electrocatalytic process, so the poisoned surface of the electrode decreased the electrocatalytic activity of the pure gold electrode. From Fig. 7, it can be seen that the continuous cyclic voltammograms of glucose on the Au/TiO₂/Ti electrode show adversary properties to that of the pure gold electrode. The oxidation peak current density of glucose is increasing in subsequent scan cycles. Possibly, the intermediates produced in the glucose electrocatalytic oxidation adsorbed

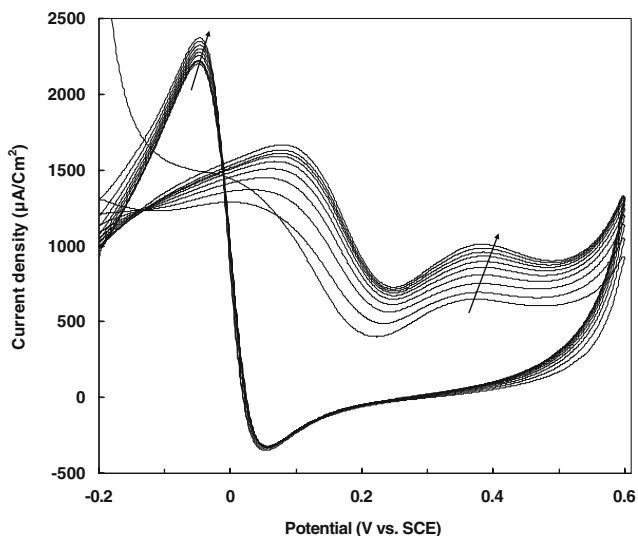


Fig. 7 The continuous cyclic voltammograms of glucose on Au/TiO₂/Ti electrode in a 1 M NaOH–0.01 M glucose aqueous solution at 25°C with a scan rate of 50 mV s⁻¹

on the electrode surface and formed an electrocatalytic active layer so increased the oxidation peak current. Compared with the gold electrode, on Au/TiO₂/Ti electrode, the complex geometry of the resulting electroactive surface (spherical-shaped deposits for Au) acts to increase the active surface area. Thus gold particles on Au/TiO₂/Ti electrode are less sensitive to the poisoning effect of strongly adsorbed species.

Discussion on glucose electro-catalytic oxidation mechanism

To study the electro-oxidation mechanism of glucose on Au/TiO₂/Ti electrode, the cyclic voltammetric curves were recorded at different sweep rates in 1 M NaOH–0.01 M glucose solutions. The results were shown in Fig. 8. It can be seen that the peak current is proportional to the potential scan rate. To investigate the electro-catalytic reaction mechanism of glucose oxidation on Au/TiO₂/Ti electrode, diagram of peak current *i_p* versus square root of sweep rate $\nu^{1/2}$ was constructed. As known in the precondition semi-infinite linear diffusion, peak current *i_p* was related to scan rate through the following equation:

$$i_p = (2.99 \times 10^5) n(\alpha n_a)^{1/2} A C_o D_o^{1/2} \nu^{1/2} \tag{2}$$

Where, *i_p* is the peak current, ν is the scan rate, *n* is the number of electrons transferred, α is the coefficient of electron transfer, *C_o* is the bulk concentration of substrate, *D_o* is the diffusion coefficient, *A* is the electrode surface area. If the concentration *C_o* is hold constant, the peak current *i_p* is linearly proportional to the square root of sweep rate $\nu^{1/2}$. While the sweep rate is kept constant, the peak current *i_p* is linearly proportional to the concentration

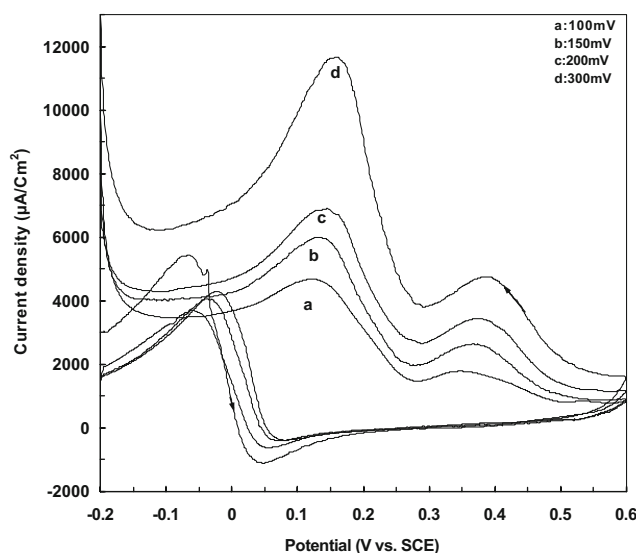


Fig. 8 The cyclic voltammograms of glucose on Au/TiO₂/Ti electrode at different scan rate

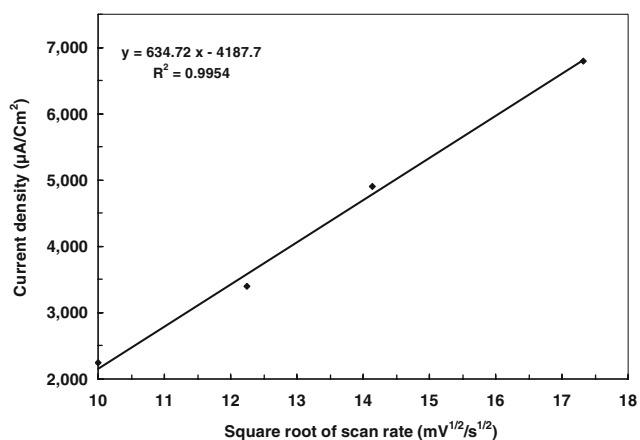


Fig. 9 The plot of glucose oxidation peak current on the Au/TiO₂/Ti electrode versus $\nu^{1/2}$

C_o , which indicates the reaction is controlled by diffusion. It is seen from Fig. 9 that the peak current i_p is linearly related to the square root of sweep rate $\nu^{1/2}$ and the correlation coefficient is $R^2=0.9954$, which ensures that the oxidation process of glucose on the Au/TiO₂/Ti electrode is controlled by diffusion.

Potential application for determination of glucose

Fig. 10 shows the cyclic voltammograms of the Au/TiO₂/Ti electrode in the presence of glucose. As can be seen in Fig. 10, Au/TiO₂/Ti electrode exhibits a well-defined catalytic oxidation current increasing linearly with an increase in the glucose concentration in range of 0.01 to 0.035 M. This Au/TiO₂/Ti electrode exhibited reproducible concentration dependence profiles for the glucose. Calibra-

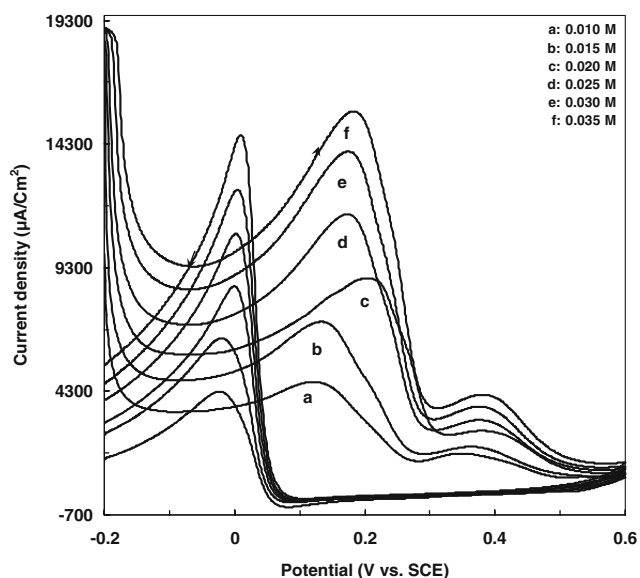


Fig. 10 The cyclic voltammograms of Au/TiO₂/Ti electrode in 1 M NaOH solution with different concentrations of glucose

tion curve for determination of glucose shows linear dependence of the anodic peak current versus glucose concentration (Fig. 11). Compared with other reports on gold nanoparticle-modified electrodes, sensitivity of glucose determination on Au/TiO₂/Ti electrode is rather low [31–33]. We can attribute this low level of sensitivity to rather larger sizes of the gold particles deposited on titanium nanotubes.

Conclusion

Au/TiO₂/Ti electrode was prepared by a two-step process consisting of anodic oxidation followed by cathodic electrodeposition. The morphology and electrocatalytic performance of the electrode was investigated by SEM and cyclic voltammetry, respectively. The results indicated that gold particles were homogeneously deposited on the surface of TiO₂ nanotubes. The electrocatalytic activity of the Au/TiO₂/Ti electrodes and pure gold toward glucose oxidation was evaluated by electrochemical voltammograms. Au/TiO₂/Ti electrodes exhibit enhanced electrochemical activity toward oxidation of glucose mainly due to the fact that deactivation process is slowed down with increasing surface roughness. Study of electro-oxidation mechanism of glucose on Au/TiO₂/Ti electrode indicated that the oxidation process is controlled by diffusion processes. Finally, the electrocatalytic oxidation peak currents for glucose exhibited a good linear dependence on concentration and therefore this modified electrode can be used for quantification determination of glucose in samples. The reason behind developing this electrode is its capability to remain unpoisoned in the presence of CO formed through oxidation of glucose thus performing as a suitable practical substrate. Also, preparation of this

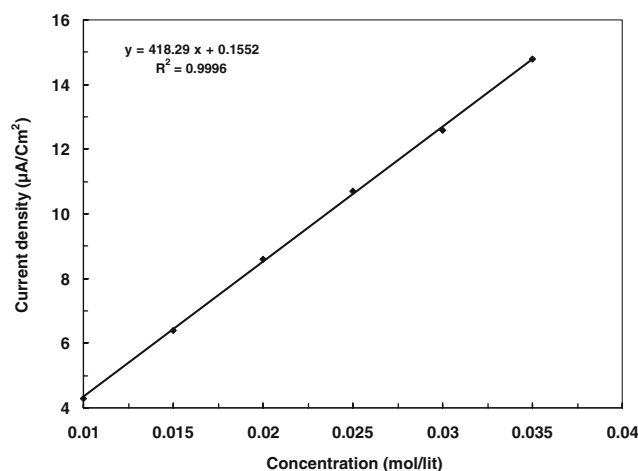


Fig. 11 The plot of glucose-oxidation peak current on the Au/TiO₂/Ti electrode versus concentration of glucose

electrode is feasible and due to the well-known biocompatibility of titanium, this sensor may be further developed to in vivo real-time and online determination of glucose.

References

1. Newman J, White S, Tothill I, Turner AP (1995) *Anal Chem* 67:4594
2. Zhao YD, Zhang WD, Chen H, Luo QM (2002) *Anal Sci* 18:939
3. Liu Y, Wang M, Zhao F, Xu ZA, Dong SJ (2005) *Biosens Bioelectron* 21:984
4. Wang J, Musameh M (2003) *Anal Chem* 75:2075
5. Wilson R, Turner AP (1992) *Biosens Bioelectron* 7:165
6. Vassilyev YB, Khazova OA, Nikolaeva NN (1985) *J Electroanal Chem* 196:105
7. Beden B, Largeaud F, Kokoh B, Lamy C (1996) *Electrochim Acta* 41:701
8. Bae IT, Yeager E, Xing X, Liu CC (1991) *J Electroanal Chem* 309:131
9. Wittstock G, Strubing A, Szargan R, Werner G (1998) *J Electroanal Chem* 444:61
10. Zhang X, Chan KY, You JK, Lin ZG, Tseung AC (1997) *J Electroanal Chem* 430:147
11. Sun Y, Buck H, Mallouk TE (2001) *Anal Chem* 73:1599
12. Park SJ, Chung TD, Kim HC (2003) *Anal Chem* 75:3046
13. Hammer B, Nørskov JK (1995) *Nature* 376:238
14. Wilson MS, Gottesfeld S (1992) *J Electrochem Soc* 139:L28
15. Pickup PG, Kuo N, Murray RW (1983) *J Electrochem Soc* 130:2205
16. Kulesza PJ, Faulkner LR (1989) *J Electroanal Chem* 259:81
17. Bose CSC, Rajeshwar K (1992) *J Electroanal Chem* 333:235
18. Bortak ED, Kazce B, Shimaze K, Kuwana T (1988) *Anal Chem* 60:2379
19. Chandler GK, Pletcher D (1986) *J Appl Electrochem* 16:62
20. Vork FTA, Barendrecht E (1990) *Electrochim Acta* 35:135
21. Bedioni F, Voision M, Derynck J (1991) *J Electroanal Chem* 297:257
22. Laborde H, Legger JM, Lamy C (1994) *J Appl Electrochem* 24:219
23. Chen KY, Tseung ACC (1996) *J Electrochem Soc* 143:2703
24. Hosseini MG, Sajjadi SAS, Momeni MM (2007) *Surf Eng* 23:419
25. Hosseini MG, Sajjadi SAS, Momeni MM (2008) *IUST Int J Eng Sci* 7:39
26. Feng D, Wang F, Chen Z (2009) *Sens Actuators B* 138:539
27. Ma Y, Di J, Yan X, Zhao M, Lu Z, Tu Y (2009) *Biosens Bioelectron* 24:1480
28. Yu JJ, Lu S, Li JW, Zhao FQ, Zeng BZ (2007) *J Solid State Electrochem* 11:1211
29. Bard AJ, Faulkner LR (2004) *Electrochemical methods fundamentals and applications*, 2nd edn. Wiley, New York
30. Gosser DK (1994) *Cyclic voltametry*. VCH, New York
31. Lin J, He C, Zhao Y, Zhang S (2009) *Sens Actuators B* 137:768
32. Ren X, Meng X, Tang F (2005) *Sens Actuators B* 110:358
33. Wang J, Wang L, Di J, Tu Y (2008) *Sens Actuators B* 135:283